Article

A New Approach to Deep Desulfurization of Light Cycle Oil over Ni₂P Catalysts: Combined Selective Oxidation and Hydrotreating

Gwang-Nam Yun [iD], Kye-Syng Cho, Yong-Su Kim and Yong-Kul Lee *[iD]

Laboratory of Advanced Catalysis for Energy and Environment, Department of Chemical Engineering, Dankook University, 126 Jukjeondong, Yongin 448-701, Korea; kwangnami@gmail.com (G.-N.Y.); kyesung@hanwha-total.com (K.-S.C.); nakimys@gmail.com (Y.-S.K.)
* Correspondence: yolee@dankook.ac.kr; Tel.: +82-31-8021-7216

Abstract: Amphiphilic phosphotungstic acid (A-PTA) and Ni₂P/SBA-15 catalysts were prepared to apply for selective oxidation of refractory sulfur compounds in light cycle oils and hydrotreating of the oxidized S compounds, respectively. Physical properties of the catalyst samples were analyzed by BET, CO uptake chemisorption, and TEM. Structural properties for the supported Ni₂P catalysts were analyzed by X-ray diffraction (XRD) and extended X-ray absorption fine structure (XAFS) spectroscopy. The selective oxidation of S compounds in the LCO feed was conducted in a batch reactor at H_2O_2/S ratio of 10, atmospheric pressure and 353 K and then the products were fed to a continuous flow fixed-bed reactor for hydrotreating at 623 K, 3.0 MPa, and LHSV's of 0.5–2.0 h^{-1}. A-PTA catalyst showed a high oxidation conversion of 95% for a real LCO feed. The following hydrotreating led to a hydrodesulfurization (HDS) conversion of 99.6% and a hydrodenitrogenation (HDN) conversion of 94.7% over Ni₂P/SBA-15, which were much higher than those of direct hydrotreating results which gave an HDS conversion of 63.5% and an HDN conversion of 17.5% based on the same LHSV of 2.0 h^{-1}. It was revealed that the reduction in refractory nitrogen compounds after oxidative treatment contributed to the increase of the following HDS activity.

Keywords: light cycle oil; selective oxidation; hydrodesulfurization; A-PTA; Ni₂P

1. Introduction

Light cycle oil (LCO) is a liquid residue of fluidized catalytic cracking process (FCC) in the petroleum industry and has been used as a blend stock for industrial fuel oil or diesel fuels. To increase its use as a value-added diesel feedstock, a severe hydrotreating is required to minimize the amounts of S, N and polycyclic aromatic compounds [1,2]. Traditionally, hydrodesulfurization (HDS) belongs to the hydrotreatment process that needs hydrogen and a catalyst to decompose the sulfur-containing compounds [1,3,4]. The units require a high capital cost and consume a large amount of hydrogen [5]. Previous studies on the HDS revealed that alkyl-dibenzithiophenes (DBT) with alkyl substitutions at four- and/or six-position are hard to completely eliminate due to a steric hindrance. These compounds are inferior in HDS reactivity and are thus classified as refractory S compounds in the conventional HDS [6–8].

Alternatives to the conventional hydrodesulfurization were introduced to overcome the low reactivity of the refractory S compounds in the HDS [9–13]. The oxidative desulfurization (ODS) has been focused extensively due to the advantages in no use of expensive hydrogen, high S selectivity, and mild reaction conditions such as an atmospheric pressure and relatively low temperatures [14–18]. Typically, the ODS is composed of two steps. The sulfur compounds in the feed are firstly oxidized to sulfones or sulfoxides, and secondly the oxidized sulfur compounds are removed by a solvent

extraction. However, a complete extraction of the sulfones is hardly achieved. Moreover, the high contents of polyaromatic compounds in LCO lead to a loss of feedstock during the extraction of sulfones [2,19].

To overcome the disadvantage of post-treatment of LCO ODS, we employed hydrotreatment after the ODS of LCO, which enabled the effective removal of refractory sulfur compounds without a loss of feedstock. The amphiphilic phosphotungstic acid catalyst (A-PTA) and the Ni_2P/SBA-15 catalysts were used for selective oxidation (OX) and the following hydrodesulfurization (HDS), respectively.

2. Results and Discussion

2.1. Physical Properties of Catalysts

Table 1 lists the physical properties of the HDS catalysts. The loadings of Ni_2P led to a reduction of the BET surface area of the supported Ni_2P catalyst samples. The spent samples showed a partial reduction in the surface area and CO uptake amount compared with the fresh samples, due to the remained reaction products on the catalysts. Table 1 also summarizes the molar ratios of Ni/Mo or P/Ni in the respective NiMo or Ni_2P samples, as analyzed by ICP-AES. Although the Ni_2P samples were synthesized with an initial P/Ni ratio of 2/1, the fresh Ni_2P sample contained lower phosphorus amounts than the original value, with P/Ni ratios of 1.115 for Ni_2P/SBA-15. A previous study has revealed that phosphorus can be removed as PH_3 during the reduction procedure [20]. During reaction, the samples could undergo further loss in P, leading to reduced P/Ni ratios, 0.838 and 0.906 for Ni_2P/SBA-15(HT) and Ni_2P/SBA-15(OX-HT), respectively, close to the stoichiometric value of 0.5 for Ni_2P.

Table 1. Physical properties of Ni_2P and NiMoS catalysts.

Samples	Conditions	BET Surface Area ($m^2\ g^{-1}$)	Pore Volume ($cm^3\ g^{-1}$)	CO Uptake ($\mu mol\ g^{-1}$)	Molar Ratios P/Ni Ni/Mo
SBA-15 support	calcined	689.1	0.92	-	-
Ni_2P/SBA-15	fresh	374.3	0.53	149	1.11
Ni_2P/SBA-15	spent (HDS)	285.6	0.39	117	0.83
Ni_2P/SBA-15	spent (ODS-HDS)	293.5	0.42	122	0.90
Al_2O_3 support	as received	101.3	0.42	-	-
$NiMo/Al_2O_3$	fresh	68.1	0.28	65	0.49
$NiMo/Al_2O_3$	spent (HDS)	59.5	0.24	30	0.49

Reaction conditions: catalyst 0.3 g (1.0 cm^3); P: 3.0 MPa; T: 653 K; LHSV: 1 h^{-1}.

Figure 1 shows the XRD patterns of the fresh and spent Ni_2P catalyst samples, as well as a bulk Ni_2P reference. The broad peak centered at 22° is typical for amorphous silica, which is observed in all samples. The diffraction pattern for Ni_2P/SBA-15 exhibits three main peaks at 40.5°, 44.8° and 47.5°, assigned to characteristic XRD peaks for a bulk Ni_2P reference. After reaction the peaks for Ni_2P phase were virtually remained with little changes in the peak positions. These results demonstrate that the Ni_2P phase is likely maintained stable under reaction.
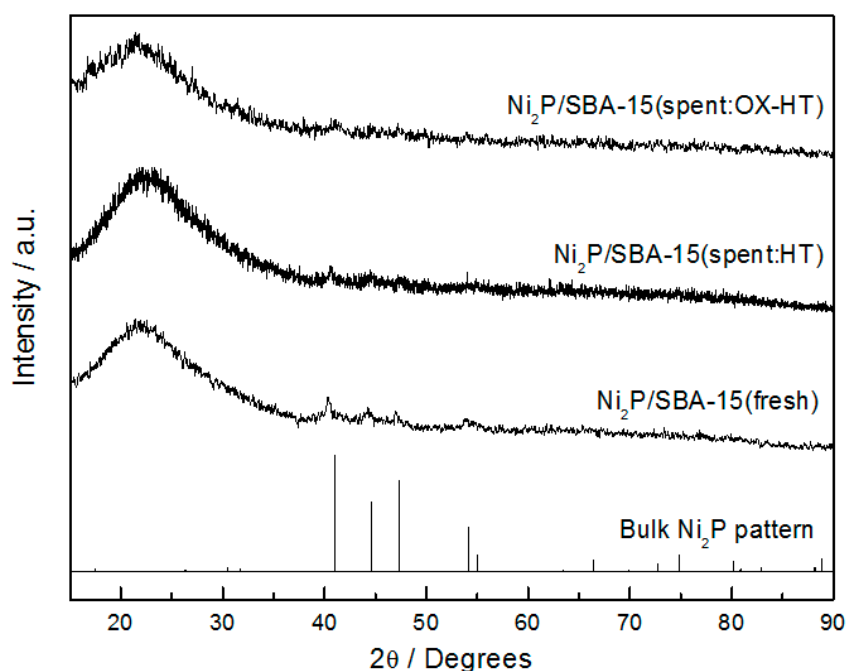
Figure 1. XRD patterns of fresh and spent Ni_2P/SBA-15 catalyst samples.

Figure 2 presents TEM micrographs of the SBA-15 support and Ni_2P/SBA-15 catalyst samples. It was observed that the SBA-15 was well synthesized with uniform hexagonal frame in pore diameter of 5 nm. The Ni_2P/SBA-15 samples retain very small Ni_2P particles smaller than 5 nm in size in the hexagonal support. The particles of Ni_2P supported on SBA-15 were regularly distributed on the support.
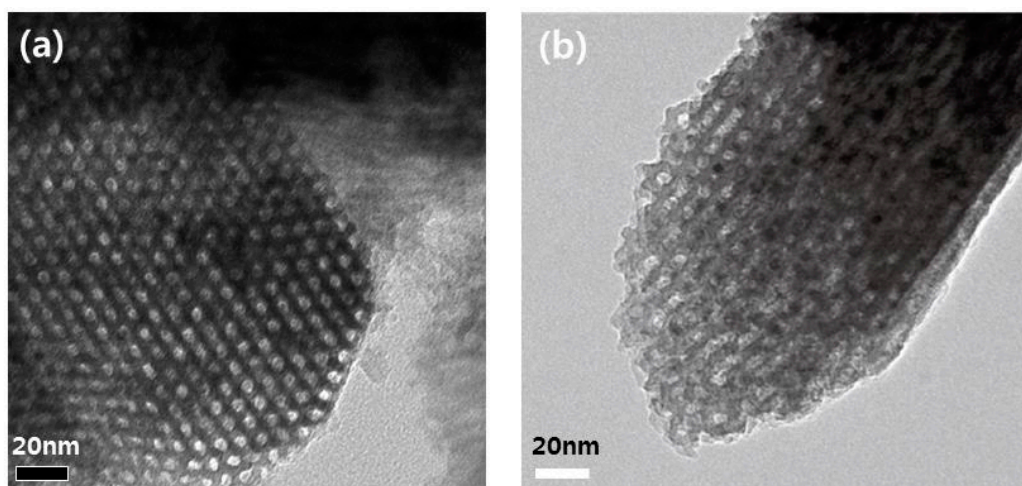

Figure 2. TEM images for (**a**) SBA-15; (**b**) Ni_2P/SBA-15 catalyst.

Figure 3 displays the Ni K-edge EXAFS spectra for a bulk reference Ni_2P sample and fresh and spent Ni_2P catalyst samples. The EXAFS spectrum for Ni_2P includes a little wider oscillation profile in 30.0–80.0 nm^{-1} assigned to Ni–P coordination and a narrower oscillation profile in 80.0–140.0 nm^{-1} to Ni–Ni coordination. This leads to the formation of two main peaks in the Fourier transforms at 0.175 and 0.240 nm, contributed to Ni–P and Ni–Ni, respectively [21]. The Fourier transforms of the fresh Ni_2P/SBA-15 catalyst sample also exhibited two main peaks at almost the same positions as

those of the bulk Ni_2P reference, demonstrating the formation of Ni_2P phase on the SBA-15 support. These results are in good accordance with the XRD results shown in Figure 1. For the spent samples, again, two distinct peaks were observed at almost the same position as the fresh samples, indicating the maintenance of Ni_2P phase during the reaction. The oscillation at 0.40–0.45 nm^{-1} became a little wider than the case of the fresh sample which implied that the spent samples were slightly bounded by sulfur or oxygen species during LCO hydrotreating.
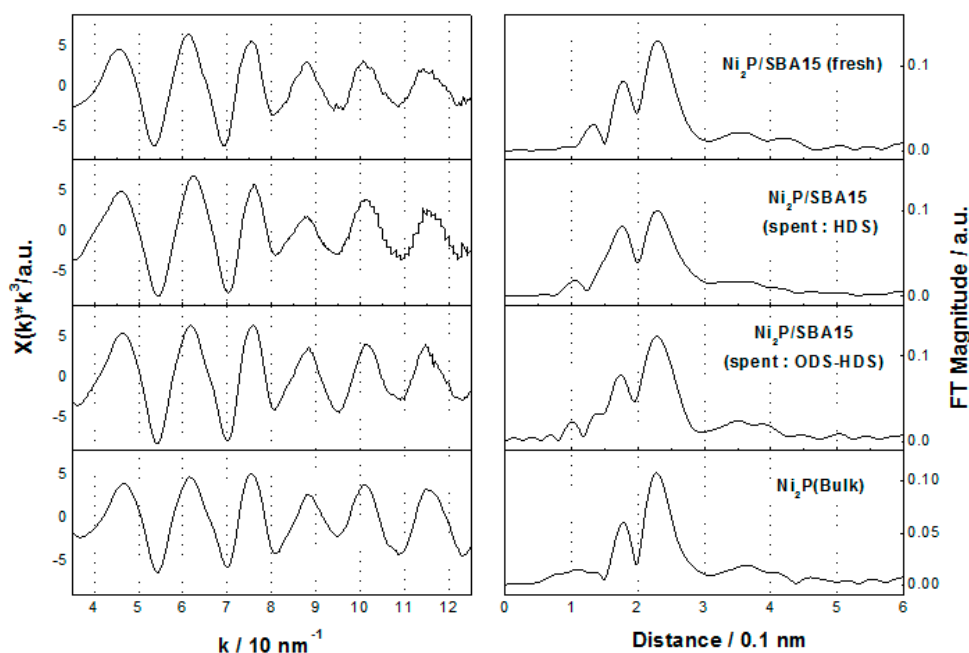

Figure 3. Ni K-edge EXAFS spectra of fresh and spent catalyst samples.

2.2. Activity Test of Catalysts

Figure 4 shows the HDS and HDN conversion of the LCO or the oxidized products at different LHSV's over the Ni_2P/SBA-15 and Ni-Mo-S catalysts. In the hydrotreating of LCO feed, the Ni_2P/SBA-15 catalyst exhibited higher activities for both HDS and HDN of 98% and 79% respectively, at an LHSV of 0.5 h^{-1} than the Ni-Mo-S catalyst with 91% for HDS and 65% for HDN at the same reaction conditions. With the increase of LHSV to 1.0 h^{-1} the Ni_2P/SBA-15 catalyst underwent a slight decrease in both HDS and HDS conversion, but Ni-Mo-S catalyst exhibited a drastic loss in the HDS and HDN conversion to give 72% for HDS and 26% for HDN. At an LHSV of 2.0 h^{-1} both Ni_2P/SBA-15 and Ni-Mo-S catalysts exhibited further loss of activity in the HDS and HDN conversion. Overall, the HDN conversion stays lower than the HDS conversion, indicating a difficulty in HDN relative to HDS as also reported in a previous work [22]. The OX-HT process is composed of two steps, including the selective oxidation followed by the hydrodesulfurization. For the OX-HT process both Ni_2P/SBA-15 and Ni-Mo-S catalysts exhibited higher activity for the HDS and HDN than the direct HT process. In particular, the Ni_2P/SBA-15 catalyst retained its high activity even under the increase of LHSV = 2.0 h^{-1}. It was noteworthy that the HDN conversion showed the considerable improvement in the OX-HT for both Ni_2P/SBA-15 and Ni-Mo-S catalysts. These results demonstrated that the OX-HT process leads to a substantial increase in the activity of HDS and HDN conversion and the reactivity of nitrogen compounds is considerably increased in comparison to the cases of HT of LCO.
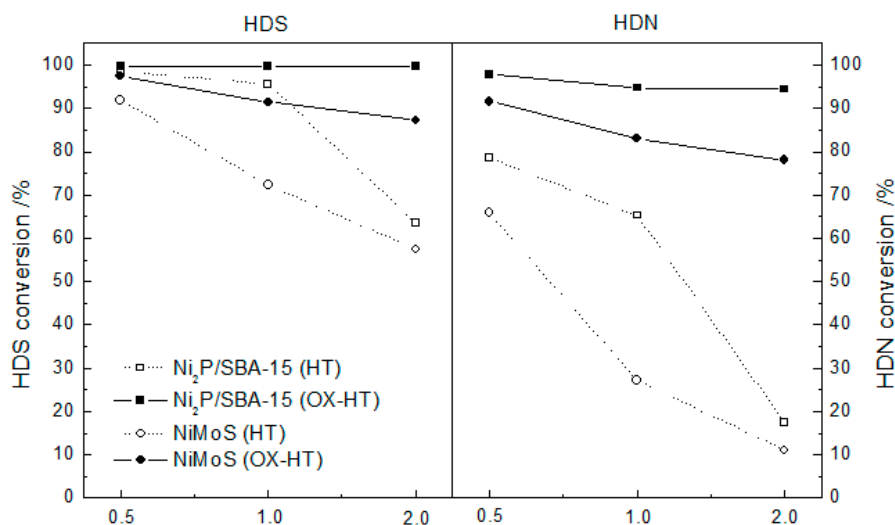
Figure 4. HDS and HDN conversions over Ni_2P/SBA-15 and Ni-Mo-S at 3.0 MPa and 623 K.

Figure 5 shows the sulfur selective GC-SCD chromatographs of the LCO feed and the reaction products after HT or OX-HT. It was observed that most of the sulfur compounds in LCO are present in the alkyl-derivatives of dibenzothiophenes, especially as methyl- or dimethyl-dibenzothiophene (C1 or C2-DBT) which are known as refractory sulfur compounds. The hydrotreating of LCO led to a removal of most BT-derivatives, while some of the DBT-derivatives remained, particularly over the Ni-Mo-S catalyst. Although the Ni_2P/SBA-15 catalyst gave rise to a better HDS activity than the Ni-Mo-S catalyst, a small amount of 4,6-DMDBT still remained, indicating the most refractory sulfur compound in the LCO. These results demonstrate that the alkyl substituents hinder the HDS over the catalyst. For the selective oxidation (OX) product, it was observed that the peaks corresponding to the DBT derivatives disappeared and new peaks corresponding to sulfones appeared at a high retention time after 20 min, whereas the peaks for BT-derivatives remained almost unchanged. As a result, the A-PTA catalyst gave the selective oxidation conversion of 95% for the real LCO feed. In the following OX-HT process the HDS conversion was much increased for both catalysts. For Ni_2P/SBA-15 the sulfur content in the product was found was very low at 14 ppm S and most refractory sulfur compounds except 4,6-DMDBT were removed during the OX-HT process, while for Ni-Mo-S catalyst alkyl-DBTs and 4,6-DMDBT remained in the product. These results demonstrated that the Ni_2P catalyst exhibits better HDS activity toward refractory S compounds than the conventional Ni-Mo-S catalyst primarily due to better HYD activity in the presence of N or aromatics than sulfide catalyst, as also reported in a previous work [21].

Generally, DBT can be oxidized to DBTS and indole is likewise oxidized to oxindole in the selective oxidation process [23]. To clarify the effect of the selective oxidation on the following hydrotreating for the LCO desulfurization, three different series of hydrotreating tests were employed over the Ni_2P/SBA-15 catalyst using different combinations of model S and N compounds such as DBT and indole, and their oxidized ones, i.e., DBT-sulfone and oxindole, as displayed in Figure 6. In the first run using DBT and indole, the HDS and HDN conversions were observed at 83.1% and 50.5%, respectively. In the presence of oxindole instead of indole, the HDS and HDN conversions were further increased to 92.2% and 80.5%, respectively. If DBT-sulfone and oxindole were fed together, the HDS and HDN conversions were further increased to 95.1% and 82.3%, respectively.
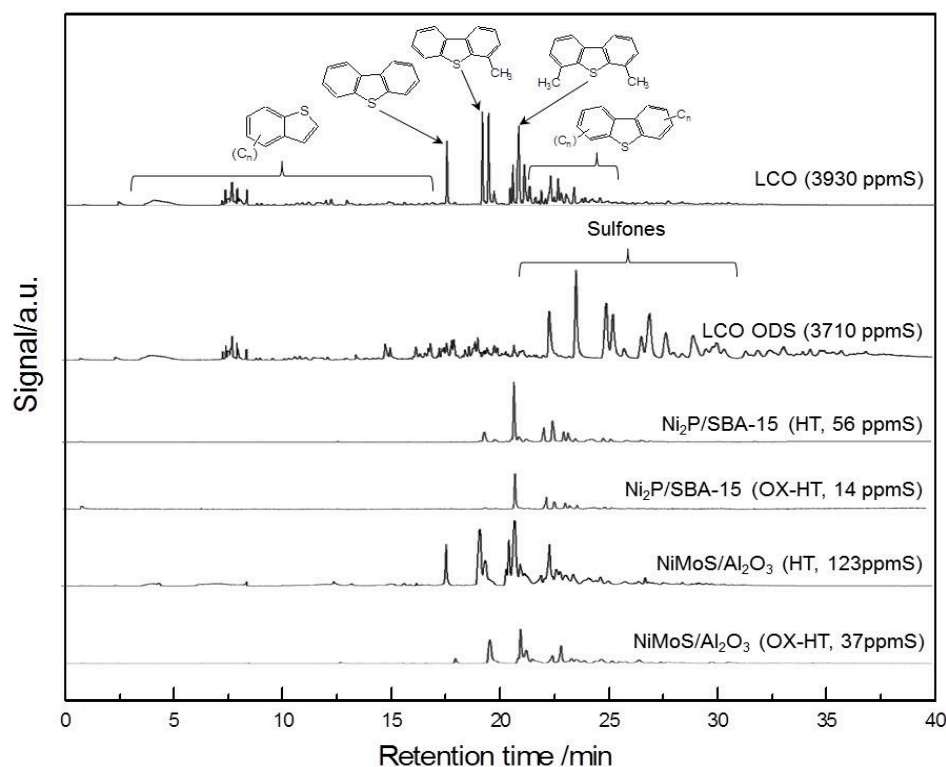
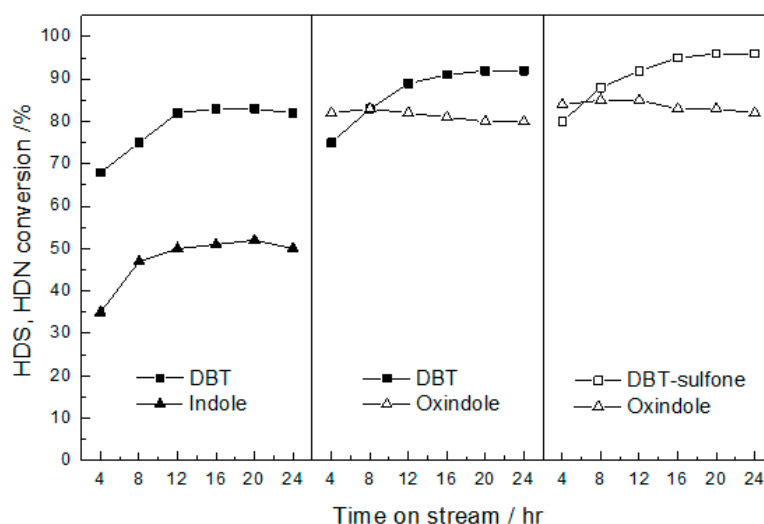**Figure 5.** GC-SCD chromatographs of LCO and reaction products.

Figure 6. HDS and HDN conversion of model S and N compounds over Ni$_2$P/SBA-15 catalyst at 3.0 MPa and 623 K.

It is noted that the HDS and HDN conversion of the oxidized sulfur and nitrogen compounds are found much higher than those of un-oxidized sulfur and nitrogen compounds as illustrated in Figure 7. Moreover, indole is found more inhibitive in the HDS of DBT than oxindole. These results thus demonstrated that the enhanced desulfurization capacity using continuous OX-HDS process is attributed to the formation of oxidized N compounds which are less inhibitive in the HDS than the original N compounds.
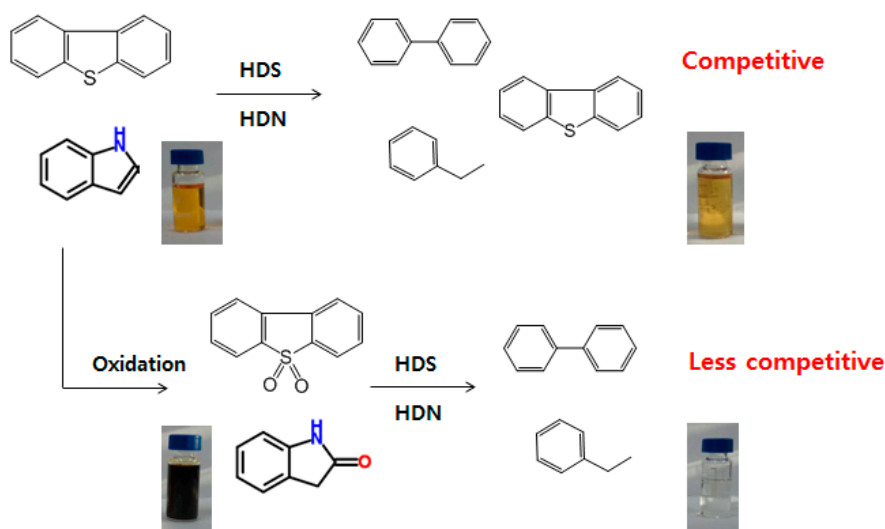
Figure 7. Proposed reaction pathways of HDS and OX-HDS.

3. Experimental

3.1. Preparation of the Amphiphilic Catalyst

The amphiphilic catalyst was prepared from a solution of trimethylammonium chloride (3.0 mmol, Alfa Aesar, 96%, Haverhill, MA, USA) and phosphotungstic acid (1.0 mmol, Alfa Aesar) in 40 mL ethanol at 338 K. Then a white precipitate was formed. After stirring for 2 h, the obtained mixture was filtered and dried at 358 K for 10 h. The resulting catalyst denoted as A-PTA.

3.2. Synthesis of Ni_2P and Ni-Mo-S Catalysts

A mesoporous SBA-15 silica support was prepared based on a literature procedure [24,25]. The Ni_2P/SBA-15 catalysts were synthesized by incipient wetness impregnation technique using aqueous metal phosphate precursors, followed by temperature programmed reduction (TPR) in flowing hydrogen. The Ni/P ratio of 1/2 was fixed in the precursors. The amount of Ni loading of 1.5 mmol/g of support was fixed at. Nickel nitrate, $Ni(NO_3)_2 \cdot 6H_2O$ (Alfa Aesar, 98%) and ammonium phosphate $(NH_4)_2HPO_4$ (Samchun, 99%, Seoul, Korea,) were used to prepare a precursor solution for impregnation, followed by drying at 393 K for 7 h and calcination at 673 K for 4 h. The resulting precursor phosphates were reduced to the corresponding phosphides by TPR from 298 to 873 K (at 10 K min^{-1}) in quartz U-tube reactors using hydrogen flow of 100 cm^3 min^{-1}. After reduction, the phosphides were cooled to room temperature under 100 cm^3 min^{-1} He flow and typically were passivated under 0.2% O_2/He flow (100 cm^3 min^{-1}) for 4 h. For comparison, Ni-Mo-S/γ-Al_2O_3 catalyst was also prepared by incipient wetness impregnation of γ-Al_2O_3 (Alfa Aesar, 99.9%, metals basis) with an aqueous solution of $(NH_4)_6Mo_7O_{24} \cdot 4H_2O$ (Samchun, 99%) and $Ni(NO_3)_2 \cdot 6H_2O$ (Alfa Aesar, 98%). The Ni-Mo-S/γ-Al_2O_3 catalyst used in this work contained 10 wt. % Mo and 3 wt. % Ni. After the impregnation step it was dried overnight at 393 K and calcined at 773 K for 2 h. Prior to the activity test, the catalyst was sulfided at 673 K for 2 h with 100 cm^3 min^{-1} of 10% DMDS/H_2 at 1 atm.

3.3. Characterization of Catalyst Samples

The CO chemisorption uptake measurement was made on the Ni_2P catalyst samples which were re-reduced in situ under flowing H_2 (100 cm^3 min^{-1}) at 723 K for 2 h before each measurement. Pulses of 100 μL CO at room temperature (300 K) were injected to the sample to measure the CO uptake using a mass spectrometer (HP 5973 inert, Agilent Technologies, Santa Clara, CA, USA). The specific surface area of the samples was measured on a Micromeritics ASAP 2010 micropore (Norcross, GA, USA) size

analyzer using the linear portion of BET plots ($P/P_0 = 0.01$–0.10) at 77 K. The elemental analysis of the samples was measured by inductively coupled plasma-atomic emission spectroscopy (ICP-AES) (Perkin-Elmer, Model Optima-4300 DV, Waltham, MA, USA). HR-TEM images were obtained using a JEM-2100F, 200 kV microscope. TGA measurements were carried out on a SDT 2960 (TA Instruments, New Castle, DE, USA) and alumina pans. About 10 mg of each sample was equilibrated at 313 K for 5 min and then heated from 313 K to 1063 K with a heating rate of 10 K min^{-1}. X-ray absorption spectroscopy for the Ni_2P catalysts were measured at the Ni K edge (8.333 keV) in the energy range 8.233–9.283 keV at the synchrotron beamline 10C of the Pohang Light Source (PLS). Detailed procedure on the XAS measurements followed our previous work [1]. The XAS data were converted using a software Winxas version 3.1.

3.4. Activity Tests

The catalytic tests of selective oxidation (OX) were performed in a three-necked glass reactor (150 mL) equipped with condenser, temperature controller, and mechanical stirrer. The LCO feed was supplied from a refinery in Korea, and the specification is given in Table 2. In a typical oxidative treatment, the LCO feedstock of 30 g was first heated to 353 K. The prepared A-PTA catalyst of 1.0 g was added to the LCO. Then, 3.0 mL of H_2O_2 (35%) was added to start the reaction. After the resulting mixture was stirred for 3 h at the reaction temperature, the product mixture was centrifuged to separate the catalyst and liquid products.

Table 2. Specifications of light cycle oil (LCO).

Physical Properties		LCO
S/ppm		3930
N/ppm		550
Color (ASTM)		L2.5
Aromatics/wt. %	Total	74.3
	Mono	14.3
	Di	40.6
	Tri+	19.4
Cetane Index		24.9
Distillation/K	IBP/5/10	498/529/535
	30/40/50	557/565/581
	60/90/95	598/671/-
	EP	-

The S compounds in the reaction products were quantified with a Hewlett Packard 6890N gas chromatograph, equipped with a sulfur chemiluminescence detector (Agilent-355 SCD, HP-1, Cross linked methyl silicone gum, 25 m $\times$ 0.32 mm $\times$ 0.17 μm).

The activity tests for hydrodesulfurization were carried out in a continuous-flow reactor (catalyst loaded with 1.0 mL) at 623 K, 3.0 MPa H_2, and a liquid hourly space velocity of 0.5–2 h^{-1}. Before injecting the reactant, the Ni_2P catalysts were activated in situ with 100 cm^3 min^{-1} of H_2 (99.999%) flow for 2 h at 723 K to remove the oxygen from the surface. The liquid reactant obtained from the oxidative treatment of LCO was fed to the reactor by means of a liquid pump along with 500 cm^3 min^{-1} H_2 flow. Liquid product compositions were analyzed at 4 h intervals. Both sulfur and nitrogen were quantified in an Antek 9000 NS analyzer (Houston, TX, USA). The conversions for HDS and HDN were defined as percent of total S and N removed from the original S and N in the LCO.

Model HDS tests using dibenzothiophene (DBT) or DBT-sulfone of 3000 ppm S in tridecane as a solvent with indole or oxindole of 500 ppm N were also performed at 623 K, 3.0 MPa H_2, and a liquid hourly space velocity of 2.0 h^{-1}.

4. Conclusions

The combined sulfur removal process of selective oxidation followed by hydrodesulfurization was employed for the desulfurization of light cycle oil (LCO). The amphiphilic phosphotungstic acid catalyst (A-PTA) showed a high activity in the selective oxidation of sulfur compounds into sulfones in LCO with the oxidation conversion of 95%. In the following hydrotreating process, it was noted that the Ni_2P/SBA-15 catalyst exhibited better HDS and HDN conversion at 99.6% and 94.4%, respectively, than the Ni-Mo-S catalyst at 97.5% and 91.6% for HDS and HDN, respectively. A model reaction test using indole and dibenzothiophene as model N and S compounds revealed that both N and S compounds undergo oxidation respectively to oxindole and dibenzothiophene sulfoxide (DBTS). Oxindole was found less inhibitive in the HDS than indole. Therefore, it was demonstrated that the selective oxidation of the refractory S and N compounds in heavy oils has a beneficial effect on the following HDS with reducing the competitive reaction by N compounds.

Author Contributions: Y.-K.L. conceived and designed the experiments; G.-N.Y. and K.-S.C. performed the experiments; Y.-S.K. contributed analysis tools; G.-N.Y. and Y.-K.L. wrote the paper.

Conflicts of Interest: The authors declare no conflict of interest. The funding sponsors had no role in the design of the study; in the collection, analyses, or interpretation of data; in the writing of the manuscript, and in the decision to publish the results.

References

1. Yun, G.N.; Lee, Y.K. Dispersion effects of Ni_2P catalysts on hydrotreating of light cycle oil. *Appl. Catal. B Environ.* **2014**, *150*, 647–655. [CrossRef]
2. Cho, K.S.; Lee, Y.K. Effects of nitrogen compounds, aromatics, and aprotic solvents on the oxidative desulfurization (ODS) of light cycle oil over Ti-SBA-15 catalyst. *Appl. Catal. B Environ.* **2014**, *147*, 35–42. [CrossRef]
3. Breysse, M.; Djega-Mariadassou, G.; Pessayre, S.; Geantet, C.; Vrinat, M.; Pérot, G.; Lemaire, M. Deep desulfurization: Reactions, catalysts and technological challenges. *Catal. Today* **2003**, *84*, 129–138. [CrossRef]
4. Song, C. An overview of new approaches to deep desulfurization for ultra-clean gasoline, diesel fuel and jet fuel. *Catal. Today* **2003**, *86*, 211–263. [CrossRef]
5. Ma, X.; Sakanishi, K.; Mochida, I. Hydrodesulfurization reactivities of various sulfur compounds in diesel fuel. *Ind. Eng. Chem. Res.* **1994**, *33*, 218–222. [CrossRef]
6. Babich, I.; Moulijn, J. Science and technology of novel processes for deep desulfurization of oil refinery streams: A review. *Fuel* **2003**, *82*, 607–631. [CrossRef]
7. Schulz, H.; Böhringer, W.; Waller, P.; Ousmanov, F. Gas oil deep hydrodesulfurization: Refractory compounds and retarded kinetics. *Catal. Today* **1999**, *49*, 87–97. [CrossRef]
8. Manoli, J.-M.; Da Costa, P.; Brun, M.; Vrinat, M.; Maugé, F.; Potvin, C. Hydrodesulfurization of 4, 6-dimethyldibenzothiophene over promoted (Ni, P) alumina-supported molybdenum carbide catalysts: Activity and characterization of active sites. *J. Catal.* **2004**, *221*, 365–377. [CrossRef]
9. Gomez, E.; Santos, V.E.; Alcon, A.; Martin, A.B.; Garcia-Ochoa, F. Oxygen-uptake and mass-transfer rates on the growth of pseudomonas p utida cect5279: Influence on biodesulfurization (BDS) capability. *Energy Fuels* **2006**, *20*, 1565–1571. [CrossRef]
10. Zhou, A.; Ma, X.; Song, C. Effects of oxidative modification of carbon surface on the adsorption of sulfur compounds in diesel fuel. *Appl. Catal. B Environ.* **2009**, *87*, 190–199. [CrossRef]
11. Zhang, J.; Wang, A.; Li, X.; Ma, X. Oxidative desulfurization of dibenzothiophene and diesel over [bmim] 3 pmo 12 O 40. *J. Catal.* **2011**, *279*, 269–275. [CrossRef]
12. Zhu, W.; Li, H.; Jiang, X.; Yan, Y.; Lu, J.; Xia, J. Oxidative desulfurization of fuels catalyzed by peroxotungsten and peroxomolybdenum complexes in ionic liquids. *Energy Fuels* **2007**, *21*, 2514–2516. [CrossRef]
13. Huang, C.; Chen, B.; Zhang, J.; Liu, Z.; Li, Y. Desulfurization of gasoline by extraction with new ionic liquids. *Energy Fuels* **2004**, *18*, 1862–1864. [CrossRef]

14.	Yan, X.-M.; Su, G.-S.; Xiong, L. Oxidative desulfurization of diesel oil over ag-modified mesoporous HPW/SiO$_2$ catalyst. *J. Fuel Chem. Tech.* **2009**, *37*, 318–323. [CrossRef]

15.	Qiu, J.; Wang, G.; Zeng, D.; Tang, Y.; Wang, M.; Li, Y. Oxidative desulfurization of diesel fuel using amphiphilic quaternary ammonium phosphomolybdate catalysts. *Fuel Process. Technol.* **2009**, *90*, 1538–1542. [CrossRef]

16.	Toteva, V.; Georgiev, A.; Topalova, L. Investigation of the oxidative desulfurization of lco model mixture by GC-MS and FTIR spectroscopy. *Fuel Process. Technol.* **2012**, *101*, 101–105. [CrossRef]

17.	Haw, K.-G.; Bakar, W.A.W.A.; Ali, R.; Chong, J.-F.; Kadir, A.A.A. Catalytic oxidative desulfurization of diesel utilizing hydrogen peroxide and functionalized-activated carbon in a biphasic diesel–acetonitrile system. *Fuel Process. Technol.* **2010**, *91*, 1105–1112. [CrossRef]

18.	Bakar, W.A.W.A.; Ali, R.; Kadir, A.A.A.; Mokhtar, W.N.A.W. Effect of transition metal oxides catalysts on oxidative desulfurization of model diesel. *Fuel Process. Technol.* **2012**, *101*, 78–84. [CrossRef]

19.	Yun, G.N.; Lee, Y.K. Beneficial effects of polycyclic aromatics on oxidative desulfurization of light cycle oil over phosphotungstic acid (PTA) catalyst. *Fuel Process. Technol.* **2013**, *114*, 1–5. [CrossRef]

20.	Oyama, S.T.; Wang, X.; Lee, Y.-K.; Bando, K.; Requejo, F. Effect of phosphorus content in nickel phosphide catalysts studied by xafs and other techniques. *J. Catal.* **2002**, *210*, 207–217. [CrossRef]

21.	Lee, Y.-K.; Oyama, S.T. Bifunctional nature of a SiO$_2$-supported Ni2P catalyst for hydrotreating: EXAFS and FTIR studies. *J. Catal.* **2006**, *239*, 376–389. [CrossRef]

22.	Infantes-Molina, A.; Cecilia, J.; Pawelec, B.; Fierro, J.; Rodríguez-Castellón, E.; Jiménez-López, A. Ni$_2$P and CoP catalysts prepared from phosphite-type precursors for hds–hdn competitive reactions. *Appl. Catal. A Gen.* **2010**, *390*, 253–263. [CrossRef]

23.	Ishihara, A.; Wang, D.H.; Dumeignil, F.; Amano, H.; Qian, E.W.H.; Kabe, T. Oxidative desulfurization and denitrogenation of a light gas oil using an oxidation/adsorption continuous flow process. *Appl. Catal. A Gen.* **2005**, *279*, 279–287. [CrossRef]

24.	Zhao, D.; Huo, Q.; Feng, J.; Chmelka, B.F.; Stucky, G.D. Nonionic triblock and star diblock copolymer and oligomeric surfactant syntheses of highly ordered, hydrothermally stable, mesoporous silica structures. *J. Am. Chem. Soc.* **1998**, *120*, 6024–6036. [CrossRef]

25.	Bérubé, F.; Kaliaguine, S. Calcination and thermal degradation mechanisms of triblock copolymer template in sba-15 materials. *Microporous Mesoporous Mater.* **2008**, *115*, 469–479. [CrossRef]